ON-DEMAND, HEATLESS EJECTION OF SUB-MM-SIZED LIQUID DROPLETS

Yongkui Tang, Lingtao Wang, Yufeng Wang, and Eun Sok Kim*
Department of Electrical Engineering-Electrophysics
University of Southern California, Los Angeles, CA 90089-0271, USA

ABSTRACT

This paper reports a nozzle-less, heatless droplet ejector capable of ejecting large liquid droplets of 460 µm in diameter with a volume of 51 nL. The ejector is built on a 1 mm thick lead zirconate titanate (PZT) sheet covered by Fresnel acoustic lens formed with annular rings of air cavities. With 450 V_{pp} pulsed 2.2 MHz sinusoidal drive, the ejector produces a focused high-intensity acoustic beam at the top surface of liquid contained in a reservoir, and is able to eject liquid droplets from the liquid surface located 10 mm away from the ejector. The ejector consistently ejects one droplet per pulse with a driving pulse width of 18.18 µs, and the highest ejection rate is estimated to be 222 Hz. When the ejector is driven with a pulse of 81.81 µs width, the ejected droplet travels 30 cm upwards before falling down due to gravity and the corresponding initial velocity of the ejected droplet is calculated to be 2.42 m/s.

INTRODUCTION

Droplet ejectors capable of ejecting large sub-mm-sized droplets have broad application potentials in biomedical fields such as drug/gene delivery, *in situ* DNA/protein synthesis, etc. Such ejectors, especially if they are capable of ejecting droplets at an electrically-tunable angle, offer unique opportunities in mid-air merging of droplets for non-contact mixing and biochemical reactions. All the commercial droplet ejectors are currently based on droplet-forming nozzles, which tend to get clogged with viscous liquid or particle-containing liquid which is commonly used in biomedical applications, causing reliability problems and increasing maintenance cost. Some of the commercial ejectors use air bubbles formed through rapid heating (which is not acceptable to many biochemical solutions), while some others use membrane deflection to push liquid out of a nozzle to eject liquid droplets. No matter which driving mechanism is used, the ejection direction of a nozzle-based droplet ejector will always be limited at the perpendicular direction to the nozzle plane, unless some special arrangement(s) is incorporated near the nozzle. Thus, nozzle-less and heatless droplet ejections are highly desirable, and have been demonstrated with focused acoustic beam generated by our self-focusing acoustic transducers (SFAT) [1-6]. However, the previously demonstrated acoustic droplet ejectors were all for small droplet size (5 – 120 µm in diameter, which corresponds to 0.065 pL – 0.91 nL in volume) and short focal length (0.4 – 0.8 mm), and are not suitable for applications that require large droplets for high throughput or synthesis through mid-air merging of droplets. To address these issues, we recently designed and fabricated a SFAT out of 1 mm thick PZT substrate with air-cavity-based acoustic reflectors for 460 µm droplet size and 10 mm focal length out of 2.2 MHz acoustic waves.

DEVICE DESIGN

As shown in Fig. 1, the transducer is built on a 1 mm thick PZT sheet (of which the fundamental thickness-mode resonant frequency is 2.2 MHz), which is sandwiched by two nickel electrodes. Over the top nickel electrode are annular-ring air cavities formed with and sealed in Parylene. The radii of the annular rings are designed into Fresnel half-wavelength band sources for 10 mm focal length. The radius of the n^{th} Fresnel band is given by [7]:

$$R_n = \sqrt{n\lambda \times (F + \frac{n\lambda}{4})} \quad (1)$$

where λ is the wavelength in the medium (in our case, water), while F is the designed focal length (10 mm).

Due to acoustic impedance mismatch between solid and air, acoustic waves which contribute to destructive interference are reflected back by the air-cavity rings, while the waves in the non-air-cavity areas propagate through the Parylene layer, and interfere constructively at the designed focal point, producing acoustic intensity high enough to overcome the surface tension and eject droplets, as illustrated in Fig. 1.

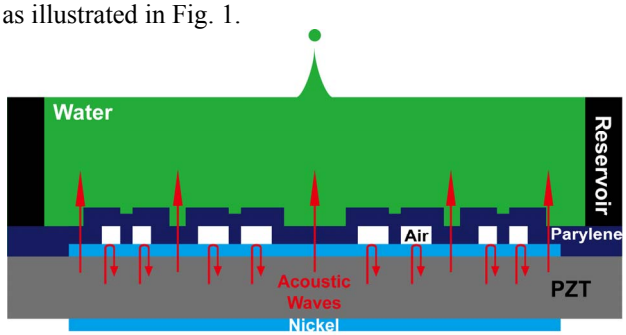

Figure 1: Schematic cross-sectional view of the device, showing how the annular-ring air reflectors work.

To verify the design, MATLAB simulation has been done to show the distribution of vertical particle displacement on both the focal plane (i.e., the xy plane at z = 10 mm) (Fig. 2a) and the central vertical plane perpendicular to the transducer at (i.e., in the xz plane at y = 0) (Fig. 2b). From both figures, we can clearly see significant focusing effect at the designed focal point with over 5 times larger particle displacement. The focal spot at the focal plane is circular with about 0.5 mm in diameter. But the focal spot at the central vertical plane is elliptical with a longer focal size along the wave propagation direction (z) than along the x direction by a factor of more than 2. In other words, the focal depth is inherently more than twice of the diameter of the focal size at the focal plane, which provides some tolerance on the needed liquid height, as droplet ejections cause some fluctuation of the liquid level in spite of automatic liquid refill into the reservoir through a microfluidic channel.

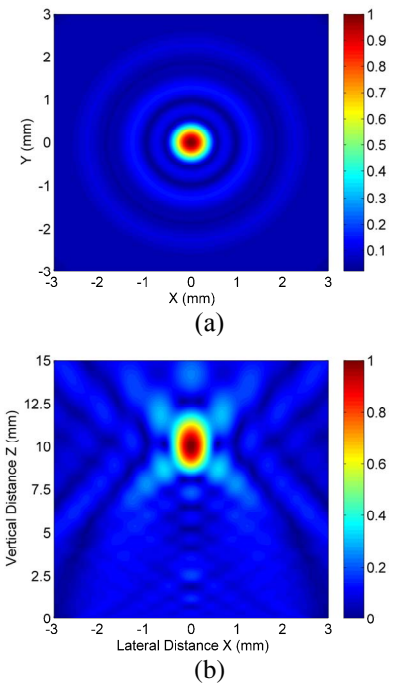

Figure 2: MATLAB simulation of the normalized vertical particle displacement at (a) the focal plane and (b) the central vertical plane perpendicular to the transducer.

FABRICATION

The device is fabricated according to the steps briefly described in Fig. 3 [6]. Firstly, predeposited front and back nickel electrodes on a 1 mm thick PSI-5H4E PZT sheet are patterned through photolithography and wet etching (Fig. 3a). The front-to-back alignment is achieved by aligning one corner of the PZT sheet to a reference corner on the masks. Then AZ 5214 photoresist is spin-coated at 1,200 rpm to form a sacrificial layer for air cavities with a thickness of around 3.5 µm, and is patterned into Fresnel half-wavelength annular rings (Fig. 3b). After that, 3.5 µm Parylene D is deposited (Fig. 3c), followed by the patterning of "release holes" through O_2 reactive ion etching (RIE) to expose the photoresist sacrificial layer (Fig. 3d), which is then removed by soaking the substrate in acetone for two days (Fig. 3e), as the acetone dissolves the photoresist sacrificial layer through the release holes. After cleaning with methanol, isopropyl alcohol (IPA) and DI water, followed by air drying, we deposit another 12.5 µm thick Parylene D to fill and seal the open holes (Fig. 3f). A photo of the fabricated ejector is shown in Fig. 4a, where the diameter of the largest annular ring is 18.8 mm.

After fabrication, an 8 × 8 cm^2 liquid reservoir (Fig. 4b) made of laser-cut acrylic sheets is attached to the fabricated device (Fig. 4a) after two wires are soldered on its top and bottom electrodes. The reservoir is designed large enough to maintain a stable water level during ejection because the relative water level change is small and ejected droplets will fall back and get collected by it. Two notches are made on two face-to-face reservoir walls and sealed by transparent tape for a brighter view during microscope observation of the ejection process. The device dimensions are listed in Table 1.

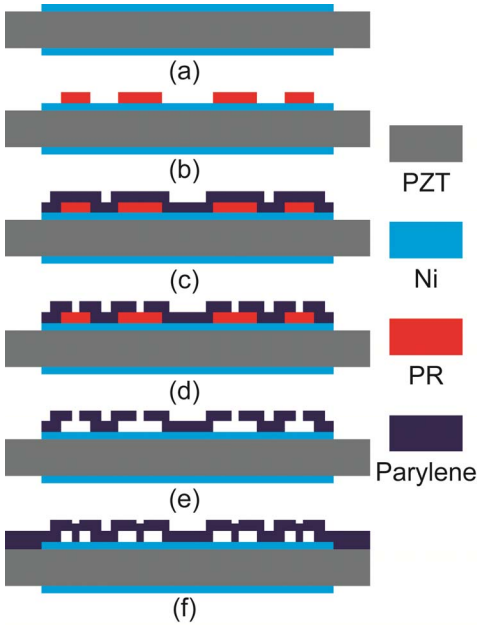

Figure 3: Fabrication process for the acoustic ejector: (a) Pattern electrodes on both sides of PZT; (b) spin-coat and pattern photoresist as sacrificial layer for air cavities; (c) deposit Parylene; (d) pattern release holes; (e) remove photoresist with acetone, clean and air dry; (f) deposit Parylene to seal the air cavities.

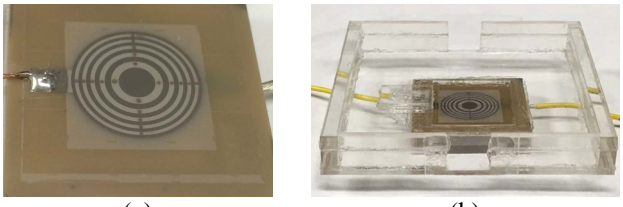

(a) (b)

Figure 4: Photos of (a) the fabricated device with air-cavity-based acoustic reflectors and (b) packaged device with acrylic liquid reservoir.

Table 1. Transducer dimensions.

PZT thickness	1.0 mm	Largest ring diameter	18.8 mm
Transducer size	3.6 x 3.6 cm^2	Reservoir size	8 x 8 cm^2
Parylene thickness	16 µm	Air cavity height	3.5 µm

RESULTS AND DISCUSSION

Measurement setup

The ejector is tested with pulsed 2.2 MHz sinusoidal signals of 450 V_{pp} at a pulse repetition frequency of 60 Hz. Triggered by a pulse generator, a function generator generates a train of sinusoidal pulses, which is then amplified by a power amplifier to drive the device. A red light-emitting diode (LED) is used as a light source to stroboscopically observe the ejection process, as the delay between device actuation and LED illumination as well as illumination duration are varied (Fig. 5). A camera attached at the end of a long-range microscope is placed at the same level of the water surface to record the ejection process to a computer.

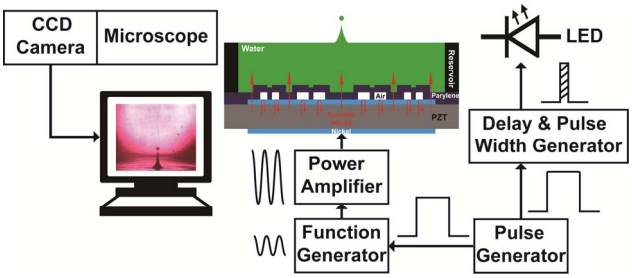

Figure 5: Measurement set-up for capturing photos of droplet ejection.

Ejection observation

When the water level is at the designed focal plane, efficient ejection of droplets is observed (Fig. 6). At the voltage level of 450 V_{pp}, a minimum of 18.18 µs (40 cycles of 2.2 MHz sinusoidal wave) pulse width is needed for ejection to happen. Figure 7 shows the time procession of the droplet ejection obtained with this minimum pulse width. From the photos we can see that a single droplet breaks off from a 1 mm height cone-shaped water column 1,000 µs after actuation, and then flies upwards. The flat water surface is recovered at around 4,500 µs which means the maximum ejection rate can be 222 Hz. The droplet diameter is measured to be 460 µm, and the volume is estimated to be 51 nL, which is 56 times larger than our previously reported value. At this pulse width, the ejected droplet travels 7 cm upward, which suggests an initial velocity of 1.17 m/s if evaporation can be ignored.

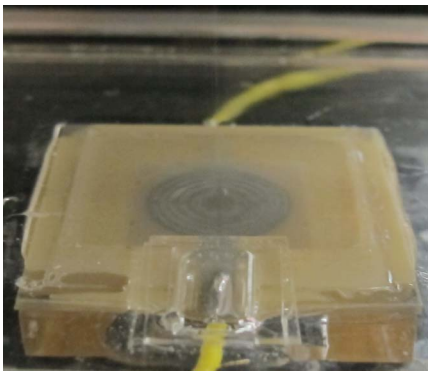

Figure 6: Photo showing a stream of droplets travelling upwards from water surface at the focal plane.

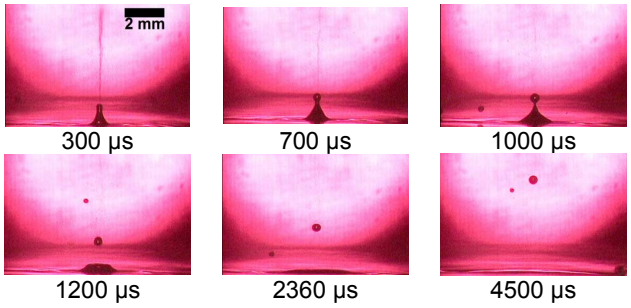

Figure 7: Photos of the ejected droplets taken with optical strobing at different time points after actuation with 18.18 µs pulse width. Smaller droplets in the background are the ones falling downward after being ejected and reaching the highest point.

To see the influence of pulse width, we observed the ejection pattern 700 µs after actuation at different pulse widths as shown in Fig. 8. From the first five photos, we can see that wider pulse width results in higher water column and faster droplet speed. However, if the pulse width is too wide, the water column turns into a strange shape with a lot of water mist being generated because of too much energy at the focal point. If we further increase the pulse width, stable droplet ejections disappear, since the vibration at the water surface is too violent. The droplets fly as high as 30 cm before falling down, when the ejector is driven with 81.81 µs pulse width. The upward traveling distance indicates an initial velocity of 2.42 m/s. Also, the droplet size is observed to be almost independent of the pulse width, confirming that the droplet size is primarily determined by the focal size at the focal plane.

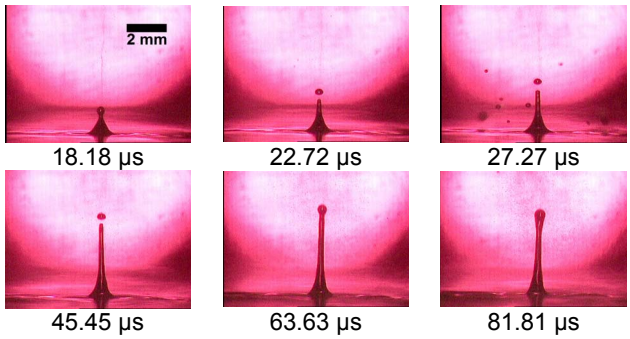

Figure 8: Photos showing ejection pattern 700 µs after actuation at different pulse widths. Smaller droplets in the background are the ones falling downward after being ejected and reaching the highest point.

We took a further look at the time procession of droplet ejection at wider pulse widths. For 22.72 µs pulse width (50 cycles of 2.2 MHz sinusoidal wave) (Fig. 9a), at 1000 µs we can see a second satellite droplet being generated due to higher energy at longer pulse width. However, as the major droplet goes up, the satellite droplet actually falls down because of its low initial speed. If we increase pulse width to 31.82 µs (70 cycles of 2.2 MHz sinusoidal wave), five satellite droplets will be generated with one droplet falling down eventually (Fig. 9b).

To conform the reliability of the device, we operated it continuously for three minutes and monitored the ejection pattern every half minute. From Fig. 10, it is clearly seen that the ejection is very stable throughout the whole process and droplet size remains the same. Water temperature is also measured before and after the operation with an infrared thermometer and we only saw a rise of 0.2 °C in temperature.

CONCLUSION

We designed and fabricated a droplet ejector based on 1 mm thick PZT substrate with Fresnel annular ring air-cavity lens for a focal length of 10 mm. Microscope observation showed stable ejection of droplets with 460 µm diameter and 51 nL volume, which are 3.8 and 56 times larger than our previously reported values, respectively. With the large focal size, this device has potential for

applications like drug/gene delivery, DNA/protein synthesis, manipulation of larger particles or even cells, treatment of cancerous cells, etc.

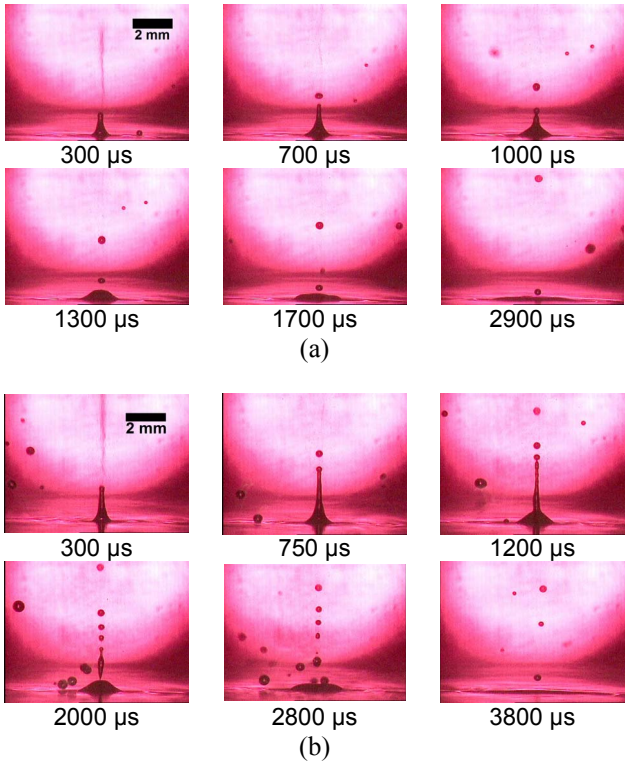

Figure 9: Photos of the ejected droplets taken with optical strobing at different time points after actuation with (a) 22.72 µs and (b) 31.82 µs pulse width showing the generation of satellite droplets at longer pulse widths. Smaller droplets in the background are the ones falling downward after being ejected and reaching the highest point.

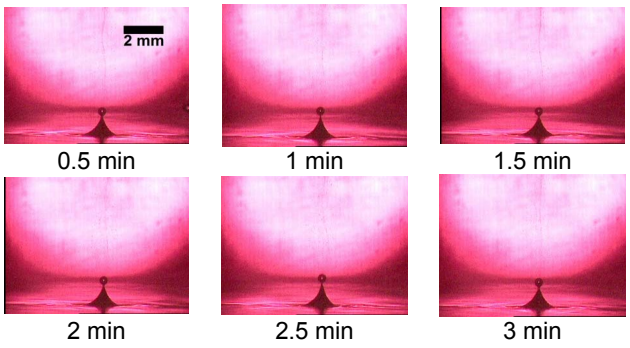

Figure 10: Photos taken at different times while droplets are continuously being ejected.

ACKNOWLEDGEMENTS

This article is based on the work supported by National Institutes of Health under grant 1R21EB022932.

REFERENCES

[1] D. Huang, E. S. Kim, "Micromachined Acoustic-Wave Liquid Ejector", *Journal of Microelectromechanical Systems*, vol. 10, no. 3, pp. 442-449, 2001.

[2] H. Yu, J. W. Kwon, E. S. Kim, "Chembio Extraction on a Chip by Nanoliter Droplet Ejection", *Lab on a Chip,* vol. 5, pp. 344-349, 2005.

[3] J. W. Kwon, H. Yu, Q. Zou, E. S. Kim, "Directional Droplet Ejection by Nozzleless Acoustic Ejectors Built on ZnO and PZT", *Journal of Micromechanics and Microengineering*, vol. 16, pp. 2697-2704, 2006.

[4] C. Lee, W. Pang, S. C. Hill, H. Yu, E. S. Kim, "Airborne Particle Generation through Acoustic Ejection of Particle-In-Droplets", *Aerosol Science and Technology*, vol. 42, pp. 832-841, 2008.

[5] C. Lee, W. Pang, H. Yu, E. S. Kim, "Subpicoliter Droplet Generation Based on a Nozzle-Free Acoustic Transducer", *Applied Physics Letters*, vol. 93, no. 034104, 2008.

[6] C. Lee, H. Yu, E. S. Kim, "Acoustic Ejector with Novel Lens Employing Air-Reflectors", in *IEEE International Micro Electro Mechanical Systems Conference*, Istanbul, Turkey, January 22-26, 2006, pp. 170-173.

[7] K. Yamada, H. Shimizu, "Planar-Structure Focusing Lens for Acoustic Microscope", *Journal of the Acoustical Society of Japan (E)*, vol. 12, no. 3, 1991.

CONTACT

*Y. Tang, tel: +1-213-447-5471; yongkuit@usc.edu